COMPARISON BETWEEN DIFFERENT LARGE-EDDY TURBULENCE MODELS IN THE SIMULATION OF SINGLE PHASE FLOWS IN A CYCLONE

Ricardo de Vasconcelos Salvo, rvsalvo@hotmail.com
Francisco José de Souza, chicao99br@gmail.com
Diego Alves de Moro Martins, moromartins@gmail.com
Aristeu da Silveira Neto, aristeus@mecanica.ufu.br
Faculdade de Engenharia Mecânica – FEMEC, Universidade Federal de Uberlândia – UFU, Av. João Naves de Ávila, 2121, Santa Mônica, Uberlândia, Brasil. Phone: +55(034) 3239-4040

Abstract. *Cyclone separators are widely used (if not, the most widely used) industrial separators devices, and can be found in a great number of different process. The separation process in these devices occurs due to the strong swirling motion of the flow, which cause the action of a centrifugal force. This force promotes the phase separation. Considering the industrial importance of these devices, Large Eddy Simulations (LES) of a single-phase turbulent flow in a model cyclone geometry were performed. The main goal of these simulations was to gather enough data, making possible the analysis of the flow field in the interior of the device, and also, of the turbulence modelling influence in an strong swirling flow. With that goal in mind, three different turbulence models - namely, the Smagorinsky subgrid model with the Van Driest wall damping function, the dynamic subgrid model and the Yakhot's RNG subgrid model were utilized. The in-house numerical code UNSCYFL3D was utilized, which is based on the finite volume technique on unstructured grids with the SIMPLE algorithm for pressure-velocity coupling. The results show similar trends for three models, comparing well to experimental data. The simulations were performed on a PC in a reasonable time frame, and the obtained results suggest that this precise methodology can be applied in a industrial frame work.*

Keywords*: Cyclone, LES, Smagorinsky subgrid model, Dynamic subgrid model, Yakhot's RNG subgrid model.*

1. INTRODUCTION

The first cyclone patent was granted in 1885 and due to their simple construction, low manufacturing cost, compactness, lack of moving parts, and relative ease of maintenance, cyclones continued to grow in popularity and improve in both construction and operation. Nowadays cyclones separators are used in a wide range of processes, ranging from food industry to oil refineries (Hoffman and Stein, 2008), where, for example, they are an essential part of the fluidized catalytic cracking (FCC) process (Hoffman et al., 2005). Along the years these devices have been the aim of several investigations, and these revealed that although the geometry of cyclones separators is simple, the flow field in their interior is extremely complex. Initially the experimental studies used intrusive probes for measuring the local flow velocity, and later breakthrough studies exclusively used optical methods, but still today most of the experimental studies only cover the influence of operating parameters or geometry changes on the separation result (Bergström and Vomhoff, 2007). In other words, many unanswered questions about the flow field in the interior of these devices remain, and optimization of cyclone performance for any given task is an oft-sought goal but is seldom achieved in practice. Understanding cyclone performance as a function of a cyclone's size, geometry, feed flow rates and the system of which it is a part is essential, and the first step to correctly do this is by understanding the gas flow in the interior of the device (Hoffman and Stein, 2008).

With this goal in mind, Large-Eddy Simulations (LES) of a single-phase, turbulent flow in model cyclone geometry were performed. The UNSCYFL3D computational code was utilized. This is a dedicated code based on the finite-volume technique with the SIMPLE algorithm for the pressure-velocity coupling on three-dimensional unstructured meshes. Three different (LES) turbulence models were used, namely: the Smagorinsky sub-grid scale model, inclunding the Van Driest wall damping function; the dynamic sub-grid model and Yakhot's RNG sub-grid model, which require no law of the wall or damping functions. Numerical results from LES on hexahedral meshes were compared with experimental data, provided by A. J. Hoekstra, showing consistent agreement for the average tangential and axial velocities. The numerical RMS values for the average tangential and axial velocities components were also compared with available experimental data, and display similar trends. Also the analysis of the instantaneous velocity fields show important aspects of this complex flow, such as secondary flows and the precessing vortex core.

All the simulations were performed using a 648.000-hexahedra grid, with a Reynolds number of 15.000. The simulations were run on a single PC in a reasonable time frame, suggesting that nowadays this precise methodology can be applied in an industrial environment.

2. MATHEMATICAL FORMULATION

The conservation of mass and the Navier-Stokes equations (conservation of momentum) for a general incompressible linear (Newtonian) viscous fluid can be written, adopting the Einstein convention, respectively as:

$$\frac{\partial u_i}{\partial x_i} = 0 \tag{1}$$

$$\frac{\partial u_i}{\partial t} + \frac{\partial}{\partial x_j}\left(u_i u_j\right) = -\frac{1}{\rho}\frac{\partial p}{\partial x_i} + \frac{\partial}{\partial x_j}\left[\nu\left(\frac{\partial u_i}{\partial x_j} + \frac{\partial u_j}{\partial x_i}\right)\right] \tag{2}$$

As far as we know, the continuity and the Navier-Stokes equations, Eq. (2) above, do apply to turbulent flow, and these equations can be modeled on digital computers, by for example, finite volume methods. Such simulations are called DNS (Direct Numerical Simulations) but, unfortunately, due to the wide range of flow scales involved, the solutions require supercomputers and even then are limited to low Reynolds numbers (White, 1991). Since the actual computation of a raw velocity component u(x,y,z,t) is not possible in high-Reynolds-number flow, the analysis of turbulent flows separates the fluctuating property from its mean value (RANS – Reynolds Average Navier-Stokes equations) or from its filtered value (LES – Large Eddy Simulations).

It is well know from literature that RANS-URANS models, except for the Reynolds Stress Models, do not apply in a proper manner to strong swirling flows (Wegner et al, 2004; Bernardo, 2005; Narasimha et al., 2006; Shalaby, 2007), when understanding the flow characteristics is the main goal. Thus, in this work, the authors considered only the LES methodology, where the filtering process of the Navier-Stokes equations can be seen as:

$$f(\vec{x},t) = \bar{f}(\vec{x},t) + f'(\vec{x},t) \tag{3}$$

The filtered part is given by:

$$\bar{f}(\vec{x},t) = \int_D f(\vec{x}',t)G(\vec{x}-\vec{x}')d\vec{x}' \tag{4}$$

And the filtering function can be defined as:

$$G(\vec{x}) = \frac{1}{\Delta_x\Delta_y\Delta_z}, \text{ if } \left|\vec{x}\right| \le \frac{\Delta}{2} \tag{5}$$

Or zero otherwise.

The filtering function define in Eq. (5) is a spatial processes, and $\Delta_{(i)}$ denotes the characteristic filter length in all three spatial directions, which determines the cut-off frequency of filtering process. Applying this process to Eq. (2) and introducing the Boussinesq hypothesis result in:

$$\frac{\partial \bar{u}_i}{\partial t} + \frac{\partial}{\partial x_j}\left(\bar{u}_i\bar{u}_j\right) = -\frac{1}{\rho}\frac{\partial \bar{p}^*}{\partial x_i} + \frac{\partial}{\partial x_j}\left[\left(\nu+\nu_t\right)\left(\frac{\partial \bar{u}_i}{\partial x_j} + \frac{\partial \bar{u}_j}{\partial x_i}\right)\right] \tag{6}$$

Where:

$$\bar{p}^* = \frac{2}{3}\rho k, \; k = \frac{1}{2}\left(\overline{u_i'u_i'}\right) \tag{7}$$

And, in Eq. (6), the turbulence viscosity (ν_t) has to be modeled.

3. TURBULENCE MODELS

3.1. Smagorinsky turbulence model

The earliest and most commonly used sub-grid scale model is the one proposed by Smagorinsky (1963) (Ferziger and Peric, 2002). Is the basis of many other more "sophisticated" models (Pope, 2003). In this model, it is assumed that the production, Eq. (8), and the dissipation, Eq. (9), of subgrid turbulent stress are equal to each other (Germano et al., 1990; Silveira-Neto, 2002).

$$\wp = 2\nu_t S_{ij} S_{ij} \tag{8}$$

$$\varepsilon = -c_l \frac{\left(\overline{u_i' u_j'}\right)^{3/2}}{l} \tag{9}$$

And the turbulent viscosity is represented by:

$$\mu_t = \rho(Cs\Delta)^2 \bar{S} \tag{10}$$

Where:

$$S_{ij} = \frac{1}{2}\left(\frac{\partial u_i}{\partial x_j} + \frac{\partial u_j}{\partial x_i}\right), \text{ and, } \bar{S} = \sqrt{S_{ij} S_{ij}} \tag{11}$$

Unfortunately, the term Cs in Eq. (10) is a parameter to be determined; it may be a function of Reynolds number and/or other non-dimensional parameters and may take different values in different flows. Normally this model requires a "pre-calibration" of the Cs term for each type of flow being simulated, which may be seen as a significant drawback of this model (Germano et al., 1990). Another difficulty associated with the utilization of this model is the fact that the turbulent viscosity does not reduce itself in near wall flows as it should. One successful recipe is to borrow the Van Driest damping, Eq. (12), which has long been used to reduce the near wall eddy viscosity in RANS models (Ferziger and Peric, 2002).

$$Cs = Cs_0\left(1 - e^{-y^+/A^+}\right)^2 \tag{12}$$

3.2. Sub-grid turbulence model from "Yakhot et al. (1986)"

Yakhot et al. (1986) have obtained a RNG subgrid scale stress model by performing recursive elimination of infinitesimal bands of small scales (Slack et al., 2000). The main difference in this model, when compared to the standard Smagorinsky model, is in the way that the total viscosity is calculated, given by:

$$\mu_{tot} = \mu\left[1 + H\left(\frac{\mu_{SGS}^2 \mu_{tot}}{\mu^3} - C\right)\right]^{1/3} \tag{13}$$

In Eq. (13) the subgrid viscosity is calculated in the same way that in the standard Smagorinsky model, Eq. (10), however in this model Cs is a theoretical constant (Cs=0.157). Also in Eq. (13) C is another constant (C=100) and H is the Heaviside Ramp function, which yields zero if the argument assume negative values. This modification in the way the total viscosity is calculated enables this model to correctly yields zero subgrid viscosity in low Reynolds number flows (for example, in near wall flows) without any ad-hoc modifications (Slack et al., 2000).

3.3. Dynamic subgrid-scale eddy viscosity model

One major drawback of the eddy viscosity subgrid-scale stress models used in large-eddy simulations is their inability to represent correctly with a single universal constant different turbulent fields in rotating or sheared flows, near solid walls, or in transitional regimes (Germano et al., 1990). Even after several authors have suggested different modifications in the original model proposed by Smagorinsky, in a way that their models presented really good results for certain applications, in a general way, those modified models did not worked quite well for flows different of these for which they were developed. Thus, although modifications of the Smagorinsky model have been successfully applied to the LES of transitional and turbulent flows, it is not possible to model effectively with a single, universal constant the variety of phenomena present in nature (Germano et al., 1990).

The dynamic SGS stress model attempts to overcome these deficiencies by locally calculating the eddy viscosity coefficient to reflect closely the state of the flow. This is done by sampling the smallest resolved scales and using this information to model the subgrid scales (Germano et al., 1990). According to Silveira-Neto (2002), two different filters are utilized:

- The grid filter, in which the grid dimensions are used to calculate its characteristic length.
- The test filter, in which a multiple of grid size, normally two, is used to calculate the characteristic length.

According to Ferziger and Peric (2002) the formulation of this model should be treated as a procedure, once it can utilize any subgrid model as a base model. A brief summary of the formulation used in this model for incompressible flows, with the modifications proposed by Lilly (1991), can be seen below.

$$C = \frac{1}{2}\left(\frac{L_{ij} M_{ij}}{M_{ij}^2} \right) \tag{14}$$

Where, C is the square of the Cs term, and:

$$M_{ij} = \left(\widetilde{\overline{\Delta}}^2 \left| \widetilde{\overline{S}} \right| \widetilde{\overline{S}}_{ij} - \widetilde{\left(\overline{\Delta}^2 \left| \overline{S} \right| \overline{S}_{ij} \right)} \right) \qquad L_{ij} = T_{ij} - t_{ij} \tag{15}$$

Where:

$$T_{ij} = \widetilde{\left(\overline{u_i u_j} \right)} - \widetilde{\overline{u}}_i \widetilde{\overline{u}}_j \qquad t_{ij} = \overline{u_i u}_j - \overline{u}_i \overline{u}_j \tag{16}$$

In the above equations the over bar denotes the grid filter process while the over tilde denotes the test filter process.

The model parameter produced by Eq. (14) is a rapidly varying function of the spatial coordinates and time so the eddy viscosity takes large values of both signs. Although a negative eddy viscosity has been suggested as a way of representing the backscatter process, if the viscosity is negative over too large a spatial region or for too long a time, numerical instability can and does occur. One way to avoid that is to use the clipping technique (stress an always positive total viscosity).

4. NUMERICAL METHOD

4.1. Numerical code

For the simulations, the computational code UNSCYFL3D (Unsteady Cyclone Flow – 3D), was used. This code has been developed as a dedicated tool for the simulation of highly rotational flows, aiming at cyclones/hydrocyclones separators and swirl tubes. It is based on the finite volume method with a CDS second order spatial scheme using the SIMPLE algorithm for the pressure correction equation on unstructured three-dimensional computational grids. Under the current implementation only hexahedral elements are used, once they are less diffusive, which is highly desirable for LES simulations. A fully implicit second order accuracy temporal scheme, three-time level is also used. The non-smoothness of the grid and non-orthogonality effects are also taken into account (Ferziger and Peric, 2002). For the solution of the linear systems the biconjugate gradient (Ferziger and Peric, 2002) and the algebraic multigrid (Notay, 2008) methods were used.

4.2. Numerical procedure

The cyclone geometry simulated, as shown in Fig. 1, is a flat bottom gas cyclone without the underflow (once only the gas phase was simulated). This geometry is the same utilized by Hoekstra et al. (1998), who kindly supplied the experimental data for comparison. In all the simulations performed the cyclone diameter was 0.1 m, and the inlet

velocity was 2.26 m/s, the density was 1.808E-05 m²/s, yielding a Reynolds number of 15000, which is the same Reynolds number of the experiments. The main differences between experiments and simulations refers to the inlet duct (considerable shorter in the simulations), the imposed velocity profile (perpendicular to the entrance for the simulations, with no imposed turbulence) and the outlet conditions (zero-gradient boundary for the simulations, whereas in the experiments it blew into free space).

For every simulation, initially a "steady state" case was run, and the resultant flow field was then used as an initial flow field for the LES simulation. This procedure considerably reduces the required time to reach a statistically established state in the LES simulations. Once this state was established the averages were gathered over a run that extended over a time period of 80 D/U_{in} (where D is the cyclones diameter and U_{in} is the velocity at the entrance of the device).

In the simulations with the Smagorinsky turbulence model, the Cs constant value was setup to Cs = 0.14, this value was obtained from previous testes with this same geometry (Salvo et al., 2009).

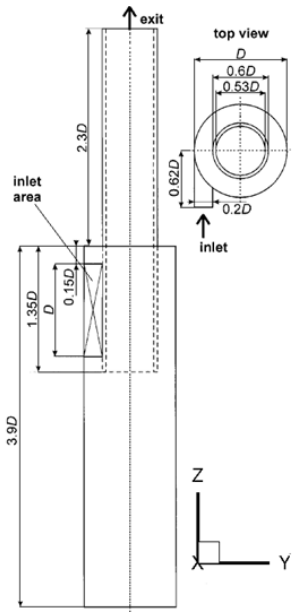

Figure 1. Model cyclone geometry simulated (Derksen and Van den Akker, 2000).

5. RESULTS

5.1. Comparison with LDA experiments

The tangential, axial, RMS tangential and RMS axial velocities profiles were analyzed in four different axial positions (Z/D = 0.89, 1.39, 1.89 and 2.39), and have been compared with LDA experimental data (provided by Hoekstra et al., 1998).

Figure 2 shows the comparison of the simulated values for the averaged tangential (Fig. 2a) and axial (Fig. 2b) velocity profiles, obtained with the three different turbulence models, and the experimental measured data. In a general way the three models performed pretty well showing consistent agreement with the experimental data. Surprisingly the results obtained with the Smagorinsky subgrid model showed an overall better agreement with the experimental data, being closely followed by the Dynamic model and then by the Yakhot RNG subgrid model, which showed some averaged tangential velocity profiles a little bit more damped than the experimental data (see Fig. 2a). It can be seen that the slope of the axial velocity component was well captured, being a little smaller in the highest section (Z/D = 0.239) than the exhibited by the experimental data. An interesting feature is the over-prediction of the axial velocity at X/D = 0.89 (first graph in Fig. 2b, from top to bottom), when the tangential velocity agrees quite well with the experimental data at this position (first graph in Fig. 2a, from top to bottom). Due to conservation of mass, this difference probably would be explained by the radial velocity component, but unfortunately this component is not explored in most articles due to the difficulties associated with its experimental measurement, as it may be almost an order of magnitude lower than the other components.

The RMS profiles (Figs. 3a and 3b) show much higher RMS values close to the center of the cyclone than near the walls. According to Derksen and Van den Akker (2000), this very likely can be attributed to the precessing vortex core. This is reinforced by the fact that the RMS values are higher at Z/D = 1.89 and 2.39 (see top two graphs in Fig 3a), which are the same regions where the precession movement is stronger .The simulated results show the same tendency as the measured data. The main differences can be seen in the results obtained with the Dynamic subgrid model for the

RMS tangential velocity profiles, most of all at the positions Z/D = 0.89 and 1.39, where a noticeble over-prediction of the measured data can be seen. This discrepancy between the results obtained with the other two models and those obtained with the dynamic model was not expected, since, at least theoretically the latter was supposed to provide the most reliable results. The reasons for this discrepancy are still being investigated by the authors, but apparently it is due to a bug in a previous version of the numerical code (the simulation with the Dynamic subgrid stress model was run in a previous version of the code, whereas the other two simulations were run in the latest version).

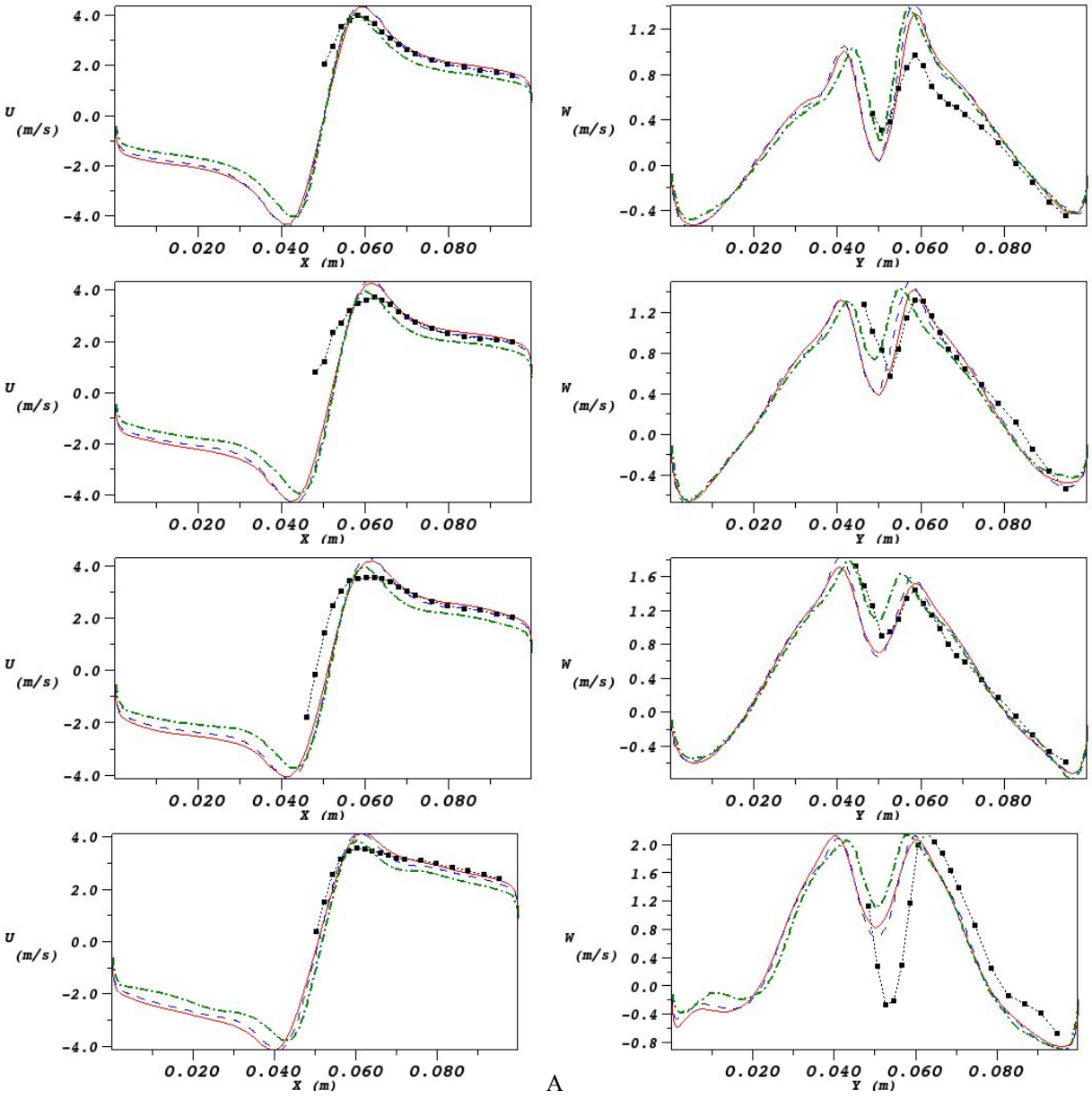

Figure 2. Averaged tangential velocity profiles (Fig. 2a) and averaged axial velocity profiles (Fig. 2b) in four different axial positions. From top to bottom, Z/D = 0.89, 0.139, 0.189 and 2.39: ···■··· Experimental; —— Dynamic subgrid stress model; – – – Smagorinsky subgrid stress model; –·– Yakhot RNG subgrid stress model.

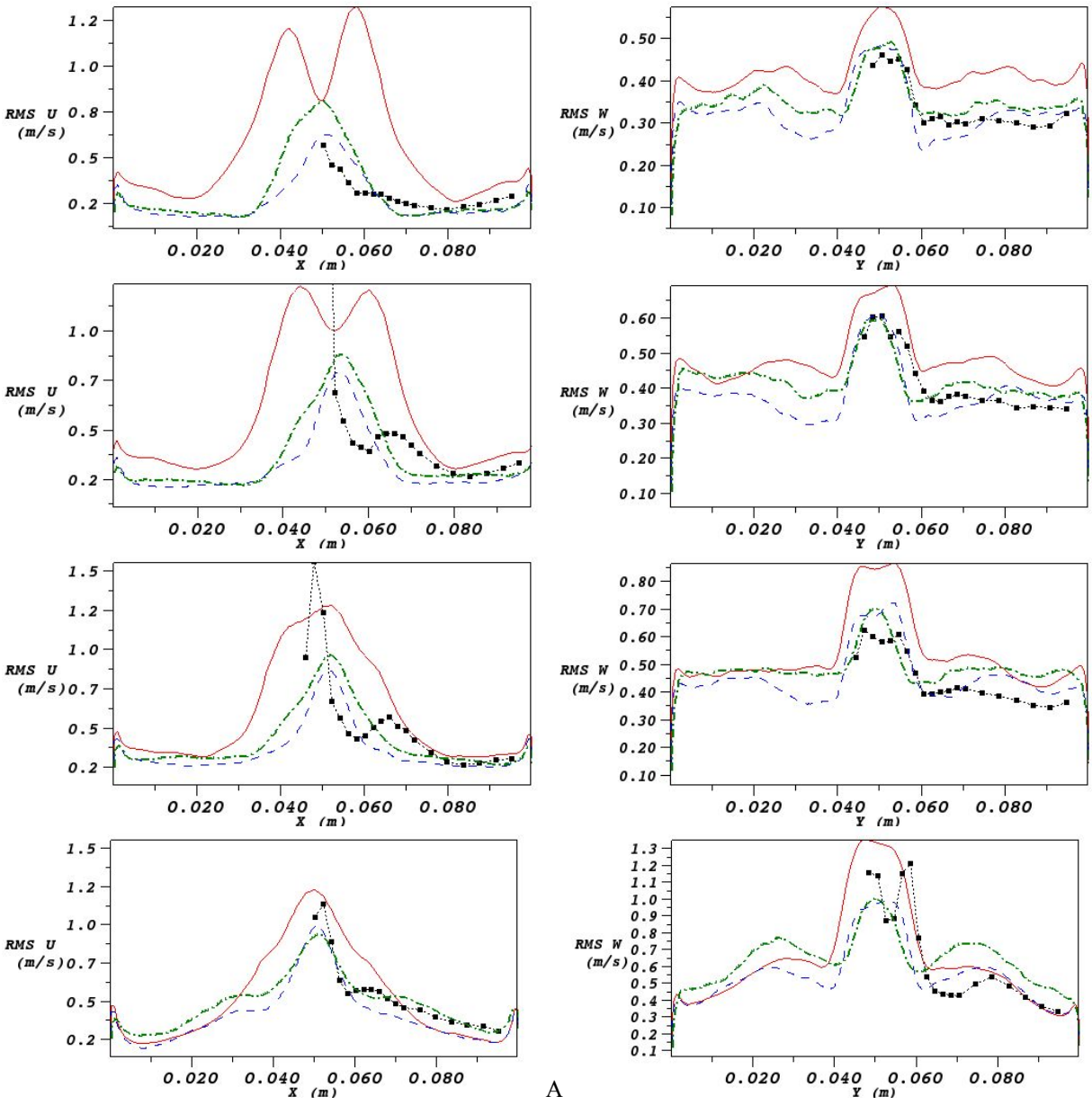

Figure 3. RMS tangential velocity profiles (Fig. 3a) and RMS axial velocity profiles (Fig. 3b) in four different axial positions. From top to bottom, Z/D = 0.89, 0.139, 0.189 and 2.39: ···■··· Experimental; —— Dynamic subgrid stress model; – – – Smagorinsky subgrid stress model; –·– Yakhot RNG subgrid stress model.

5.2. Precession vortex core

The precessing vortex core (PVC) is a hydrodynamic instability that normally occurs in highly rotating flows (Hoekstra et al., 1999) and mainly affects the core region of the flow, due to the great radial gradients of tangential and axial velocities, making the vortex core unstable. This phenomenon is normally undesirable, once it may introduce higher pressure drops (which can be directly related to higher energy consumption), mechanical vibrations, reduction in the separation efficiency among others factors (Solero and Coche, 2002).

The PVC manifests itself as a quasi-periodically fluctuating signal, for example, a velocity signal (Derksen and Van den Akker, 2000), as shown in Fig. 4. This result was obtained with the Smagorinsky LES model at the position Z/D = 1.9. This quasi-periodically fluctuating signal can be associated with a "main" frequency by means of a power spectral density function, Fig. 5. With the PVC frequency it is possible to encounter the correspondent Strouhal number St = ($f_{peak}D/U_{in}$). From Fig. 5, it is clear that the frequency peak is f_{peak} = 10.49 HZ, corresponding to a Strouhal of St = 0.465, which is in good agreement with the experimental value of St_{exp} = 0.49.

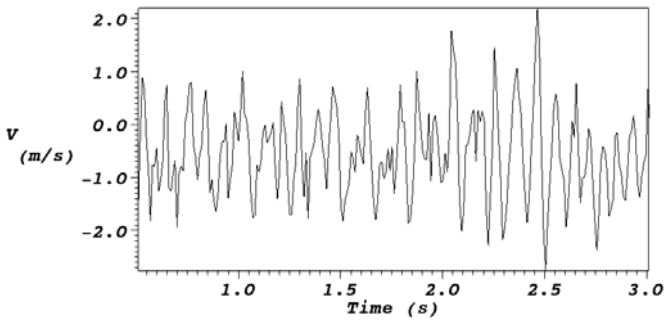

Figure 4. Radial velocity component in the position Z/D = 1.9, obtained for a time period of 2.5 seconds.

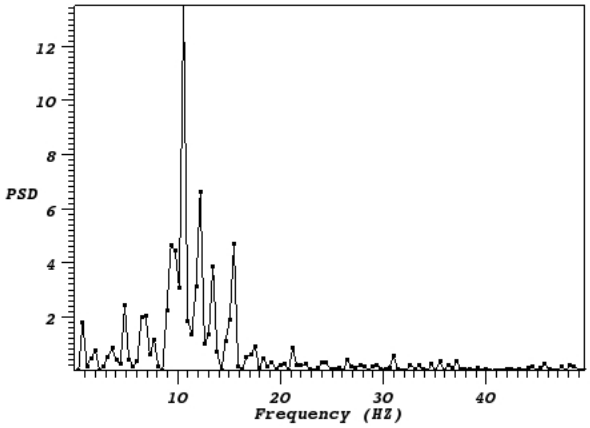

Figure 5. Power spectral density function of the radial velocity component time series presented in Fig. 4.

The center of the vortex can also be associated with the least pressure point (Derksen and Van den Akker, 2000), which allows the precession of the vortex core to be visualized by means of pressure fields along time. Fig. 6 presents series of pressure fields recorded every 0.001 seconds at the position Z/D = 1.9.

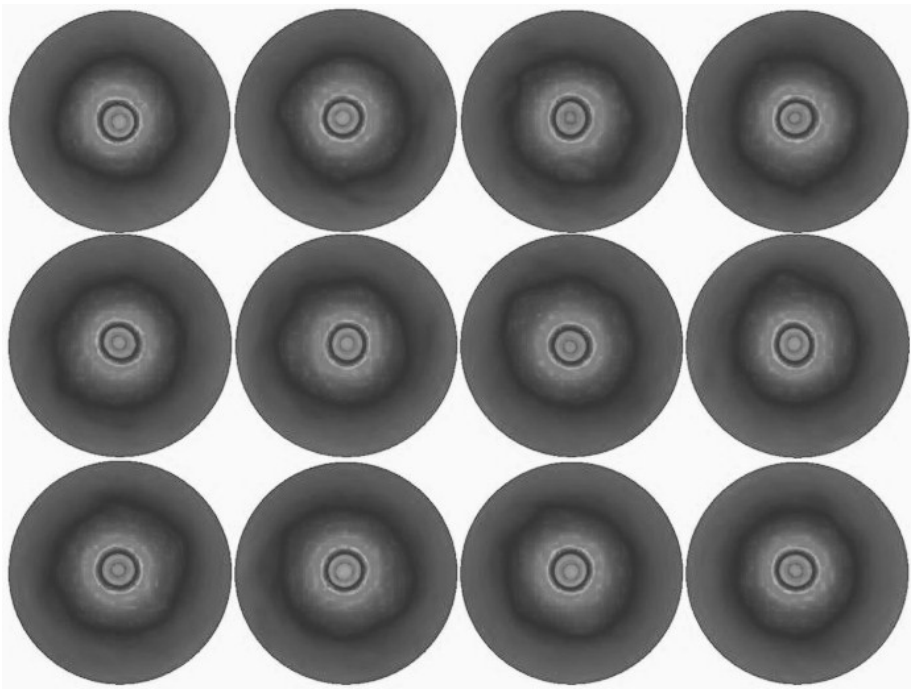

Figure 6. Pressure fields in different time steps, separated by 0.001 seconds, at plane Z/D = 1.9.

A real swirling flow normally has a core of near solid-body rotation surrounded by a region of near loss-free rotation (Hoffman and Stein, 2008). This also can be seen in Fig. 6, where the division between these two "types" of flow happens in the clearest part (outside the dark ring near the center of the cyclone) which approximately corresponds to the tangential velocity peak, as can be seen in Fig 2a, near the radial positions 0.04 and 0.06 m.

Part of the discrepancy between the results obtained with the Yakhot RNG subgrid model maybe explained by Fig. 7, in which it is clear that the Smagorinsky model "feels" the presence of the vortex core, while the Yakhot RNG model ignores it, presenting considerable changes in the turbulent viscosity only close to the walls. The explanation above raises an interesting question: why a model yielding much higher effective viscosity presents also higher values of averaged velocities, results that agree better with the experimental data? One possible explanation is based on the RMS profiles showed in Fig. 3. Since the effective viscosity is smaller in the simulations with the Yakhot RNG subgrid model, it presents higher RMS values, which may be related to a higher turbulence level and this in turn may lead to a smaller averaged velocity profile.

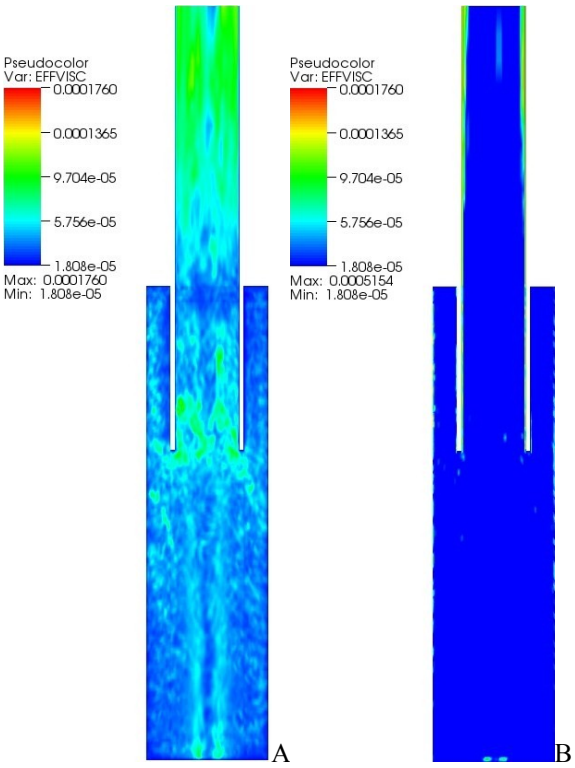

Figure 7. Transient, physical time =1.42 s, effective viscosity fields for the Smagorinsky subgrid model (a) and the Yakhot RNG subgrid model (b).

6. CONCLUSION

Large-Eddy simulations (LES) of single-phase turbulent flow in a model cyclone geometry were performed. Three different models were utilized and their influence on the results was analyzed. The obtained results surprisingly revealed that the Smagorinsky subgrid stress model was responsible for the best agreements with the experimental data and Dynamic model simulation resulted in too high RMS velocities profiles. This is still under investigation. The Yakhot RNG subgrid stress model provided lower averaged velocities profiles, and good RMS velocities profiles. One possible explanation for this is that the smaller turbulent viscosity provided by this model may be translated into a higher turbulence level, and this in turn may be responsible for a higher dissipation, leading to smaller averaged velocity values. The precessing vortex core was corrected simulated with a frequency very close to the experimental data (simulated Strouhal St = 0.46 and experimental Strouhal St_{exp} = 0.49). This demonstrates that the simulations resulted in good qualitative and quantitative agreement with the experimental data.

Although some discrepancy between the simulations results and the experimental data do exist, important flow phenomena was captured, like the precessing vortex core, showing that LES is an excellent tool in the simulation of highly swirling flows. This gives confidence to the authors to invest in this precise methodology for the simulation of highly swirling flows in the presence of a particulate phase.

7. ACKNOWLEDGEMENTS

The authors would like to thank A. J. Hoekstra for supplying the experimental data.
The authors also would like to thank FAPEMIG, CAPES, CNPQ and PETROBRAS for the financial support.

8. REFERENCES

Bergström, J. and Vomhoff, H., 2007, "Experimental hydrocyclone flow field studies", Separation and Purification Technology, Vol 53, pp. 8-20.

Bernardo, S., "Estudo dos escoamentos gasoso e gás-sólido em ciclones pela aplicação de fluidodinâmica computacional", 2005, 240 f., teses, Universidade Estadual de Campinas, Campinas, São Paulo, Brazil.

Derksen, J.J. and Van den Akker, H.E.A., 2000, "Simulation of vortex core precession in a reverse-flow cyclone", AIChE Journal, Vol 46, N° 7, pp. 1317-1331.

Ferziger, J.H. and Peric, M., 2002, "Computational methods for fluid dynamics", Springer.

Germano, M., Piomelli, U., Moin, P. and Cabot, W.H., 1990, "Adynamic subgrid-scale eddy viscosity model", American Institute of Physics, Vol 7, pp. 1760-1795.

Hoekstra, A.J., Derksen, J.J. and Van den Akker, H.E.A., "An experimental study of turbulent swirling flow in gas cyclones", Chemical Engineering Science, Vol 54, pp. 2055-2065.

Hoffman, A. C., Stein, L. E., 2008, "Gas cyclones and swirl tubes – principles, desing and operation", Second Edition, Springer – Verlag Berlin Heidelberg.

Lilly, D. K., 1992, "A proposed modification of the Germano subgrid-scale closure method", Phsics Fluids, v. 4, no 3, 633-635.

Narasimha, M., Brennan, M. and Holtham, P.N., 2006, "Large eddy simulation of hydrocyclone – prediction of air-core diameter and shape", International Journal of Mineral Processing, Vol 80, pp.1-14.

Notay, Y., 2010, "An aggregation-based algebraic multigrid method", Electronic transactions on numerical analysis, v. 37, p. 123-146.

Yakhot, A., Orszag, S. A., Yakhot, V. and Israeli, M., 1986, Renormalization group formulation of large-eddy simulation, J. Scientific Computing, v. 1, p. 1-51.

Pope, S.B., 2003, "Turbulent Flows", Cambridge University Press, 2003.

Salvo, V. R., Souza, F. J., Padilla, E. L. M., Silveira-Neto, A., "Large-eddy simualtion of single phase turbulent flows in cyclones", 20 th International Congress of Mechanical Engineering, November 15-20, 2009, Gramado, RS, Brazil.

Shalaby, H. H., "On the potential of large eddy simulation to simulate cyclone separators", 2007, 121 f., teses, Von der Fakultät für Maschinebau der Technischen Universität Chemnitz, Germany.

Silveira-Neto, A., 2002, "Turbulência nos fluidos aplicada", Faculdade de Engenharia Mecânica, Universidade Federal deUberlândia – UFU, Uberlândia, Brasil.

Slack, M.D., Prasad, R.O., Bakker, A. and Boysan, F., 2000, "Advances in cyclone modelling using unstructured grids", Institution of Chemical Engineers, Vol 78, Part A, pp. 1098-1104.

Solero, G. and Coghe, A., 2002, 'Experimental fluid dynamic characterization of a cyclone chamber", Experimental thermal science, v. 27, p. 87-96.

Wegner, B., Maltsev, A., Schneider, C., Sadiki, A., Dreizler, A., and Janicka, J., 2004, "Assessment of unsteady RANS in predicting swirl flow instability based on LES and experiments", Heat and Fluid Flow, v. 25, p. 528-536.

White, F. M., 1990, "Viscous fluid flow", McGraw-Hill.

9. RESPONSIBILITY NOTICE

The authors are the only responsible for the printed material included in this paper.